

## SUBPIXEL EDGE DETECTION IN BLURRY AND NOISY IMAGES

ANNA FABIAŃSKA\*

*Institute of Applied Computer Science, Lodz University of Technology, 18/22 Stefanowskiego Str.,  
Lodz, 90-924, Poland  
anna.fabijanska@p.lodz.pl  
http://an-fab.kis.p.lodz.pl*

This paper considers the problem of subpixel edge detection. In particular, a new reconstructive approach is introduced. The method determines subpixel edge position based on the properties of the Gaussian function used for modeling gradient profile at the edge. The results showing the robustness of the new method against averaging, Gaussian blur and Gaussian noise are presented. In all the experiments the introduced method is compared with other state-of-the-art methods of subpixel edge detection. The comparison clearly shows that the new method outperforms the existing ones.

*Keywords:* Edge detection; blurred edge; noise; subpixel accuracy; Gaussian function.

### 1. Introduction

Edge detection is a problem of crucial importance in image processing. Edges define location and geometric features of the objects present in the scene. Therefore, in a typical vision system edge detection is performed during low level processing and provides information for operations performed in the following stages, such as quantitative analysis, target recognition or image coding.

Recently, the requirements for accuracy of edge detection has been rapidly increasing. Satellite remote sensing, telemetry, photogrammetry, medical image analysis, industrial inspection, geometrical measurement and other applications where accuracy is at premium require precision of tenths or even hundredths of pixel.

The traditional, well-established methods for edge detection such as gradient operators (Sobel, Prewitt, Roberts), Canny edge detector or operator LoG all belong to the pixel level. Therefore, they are mostly insufficient for the practical applications of the modern machine vision. Due to their low precision and extracted wider edges these approaches have difficulties in meeting the actual accuracy requirements.

Therefore, the development of subpixel techniques for edge detection has become one of the hotspots of the current research in image processing. Some work has already been done on this problem. However, the major methods for subpixel edge detection are still to be developed. It should be also underlined that while there has been substantial work performed on the detection of clear and well defined edges at subpixel accuracy, little has

\* Institute of Applied Computer Science, Lodz University of Technology, 18/22 Stefanowskiego Str., Lodz, 90-924, Poland

been done on the subpixel edge detection in the low contrast images containing blurred, noisy and unsharp edges.

This paper presents a new method which is a step forward through introducing the subpixel analysis into edge detection. In particular, the method is dedicated to the precise edge detection of significantly blurred edges. As the already proposed methods deal mostly with sharp, regular and well defined edges the introduced approach can be considered novel.

This paper is organized as follows. Firstly, in Section 2 a background on subpixel edge detection is given. Then, in Section 3 the proposed method for subpixel edge detection is introduced. Section 4 presents the results of the new algorithm obtained for synthetic images. Blur resistance and noise resistance of the new method are regarded in Sec. 4.1 and Sec. 4.2 respectively. In Section 5 the results of edge detection obtained for real images are shown and discussed. Finally, Section 6 concludes the paper.

## **2. Background on Subpixel Edge Detection**

The main idea behind subpixel edge detection is to overcome limitations caused by digital raster and to determine edge location inside a pixel. However, it should be remembered that the discrete structure of a pixel grid significantly influences the shape of objects present in the image and reduces edge information. Therefore edge position inside a pixel can only be approximated with some probability.

The need of the subpixel accuracy in image processing and analysis was firstly pointed out in the late 70's [Nevtia, Babu (1978)]. Since then the issue of edge detection at subpixel level has gained an interest of scientists and researchers. Recently, subpixel approaches to edge detection can be qualified into three main groups:

- (1) moment-based methods;
- (2) reconstructive methods;
- (3) curve-fitting methods.

These methods are characterized in the following subsections.

### **2.1. Moment-Based Methods**

Moment-based methods use image moments to determine the position of the edge. Intensity moments (based only on pixel intensities) and spatial moments (which use spatial information about pixel neighborhood) can be differentiated.

The first moment-based approach to edge detection was proposed by Machuca and Gilbert [Machuca, Gilbert (1981)]. Their method integrates the region which contains the edge in order to determine edge position using moments found within the integrated region. The moments are defined based on properties of the vector from a given pixel to the center of gravity of pixel's square neighborhood.

Tabatabai and Mitchell [Tabatabai, Mitchell (1984)] proposed a method for subpixel edge detection which fits three intensity moments to the ideal step edge which is defined as sequence of intensity  $h_1$  followed by sequence of intensity  $h_2$ . The moments are defined as a sum of pixel intensity powers and do not consider any spatial information.

The main drawback to this method is that it determines edges only in non-decreasing or non-increasing sequences of intensities.

Method developed by Lyvers [Lyvers (1989)] fits spatial (geometric) moments into a new 2D model of the ideal edge. In the model the edge is described by four parameters which determine its position with subpixel accuracy. Their determination requires determination of six moments using circular masks. This makes the method computationally complex. Moreover, moments used by the method are not orthogonal what makes the method lacks optimality in information redundancy. However, the edge model put into subpixel edge detection by Lavers was used by the succeeding approaches to the considered problem. Specifically, Ghosal and Mehrotra [Ghosal, Mehrotra (1993)] proposed method which fits orthogonal Zernike moments into Lyvers' edge model. This approach decreased complexity of the method as only three masks are required. However, Zernike moments have difficulty in describing small objects.

Recently, Bin [Bin et al. (2008)] put forward orthogonal Fourier-Mellin moments (OFMM) proposed by Sheng and Shen [Sheng, Shen (1994)] into subpixel edge detection. OFMMs are also fitted into the Lyvers' edge model.

The main drawback to moment-based approaches is the lack of clear criteria for classifying pixels as edge or non-edge. Moreover, they produce response (i.e. parameters of subpixel edge) for every set of pixels containing change in image intensity and work properly only in the close neighborhood of the edge pixel. If the edge position is more distant than the dimensions of region of an integration, the moment based approaches fail. Therefore in the current form moment-based approaches can only be used to refine position of properly defined coarse edges.

## 2.2. *Reconstructive Methods*

The main idea behind the reconstructive methods to subpixel edge detection is to retrieve the continuous information of the edges from the discrete image. Therefore, these methods apply various interpolation and approximation techniques in order to reconstruct continuous image function based on discrete sample values. Image function can be reconstructed independently in vertical and horizontal direction (row by row, column by column) or simultaneously in both directions. In the first case, one dimensional image function is found in each direction. The final result is a superposition of the results obtained in each direction. In the second case, two dimensional continuous function is build. The coordinates of the characteristic points of the reconstructed image function (i.e. local extremes, zero crossings, inflection points, etc.) indicate edge position with the subpixel accuracy. The sample values of image function used for reconstruction are pixel intensities or are provided by the traditional approaches to edge detection such as Sobel, Canny or LoG.

The reconstructive approaches can be divided into the following groups:

- (1) methods reconstructing image intensity [Hagara, Kulla (2011); Xu (2009)];
- (2) methods reconstructing the first image derivative [Bailey (2005); Fabijańska(2012); Fabijańska (2014); Rocket (1999)];

- (3) methods reconstructing the second image derivative [MacVicar-Whelan, Binford (1991); MacVicar-Whelan, Binford (1981); Jin (1990)].

Methods reconstructing image intensity determine subpixel edge position based on the properties of a function modeling image intensity at the edge. As an example approach by Xu [Xu (2009)] can be given. The method approximates image intensity at the edge using the second order polynomial. Subpixel position of the edge is indicated by the point at the curve where image intensity equals to the average of intensities of the background and the object. However, methods reconstructing image intensity are in minority.

Methods reconstructing the first image derivative attempt to build the continuous image gradient function based on gradient sample values provided by operators like Sobel, Prewitt [Bailey (2005)] or Canny [Rocket (1999)]. Coordinates of the maximum of the reconstructed function indicate the edge position with the subpixel accuracy. Most commonly, the second order polynomial is fitted into gradient sample values in a small (3 - 5 pixels) neighborhood [Bailey (2005); Rocket (1999)]. Several approaches using wavelet transform instead of the first image derivative have also been proposed [Liu et al. (2004); Xu (2009b)].

Methods reconstructing the second image derivative retrieve the continuous function based on sample values provided by operator LoG. The zero-crossings of the reconstructed second image derivative function determine the edge position with the subpixel accuracy. Most commonly image derivative function is linearly interpolated in the neighborhood where the second image derivative function changes its sign [MacVicar-Whelan, Binford (1991); MacVicar-Whelan, Binford (1981)]. However, higher order polynomials are also applied [Jin (1990)].

In order to diminish the computational complexity of edge detection method, image function is often reconstructed in some neighborhood of the coarse border. Therefore, firstly, standard feature selection is applied in order to determine coarse location of the edge. Then this location is refined to the subpixel level adapting local feature pattern in the closest neighborhood.

### **2.3. Curve-Fitting Methods**

Curve-fitting methods attempt to build the continuous edge by fitting curves into edge points determined with pixel accuracy. The fitting is performed in the image plane. This methodology was used by Yao and Ju [Yao, Yu (2009)] who fitted cubic splines into spatial data points provided by Canny operator or by Breder [Breder et al. (2009)] who used B-spline interpolation. Similar approach was also proposed by Kisiworo [Kisiworo et al. (1991)] who applied deformable models for subpixel edge detection.

Curve fitting methods can be particularly useful in applications where shape of the border is known a priori. However, this group of methods is sensitive to badly defined edge points which can disturb the shape of the object.

## 2.4. Other Methods

Several approaches to subpixel edge detection which do not meet the classification presented above have also been proposed. For example, Stanke [Stanke et al. (1998)] proposed a method which determines edge location at subpixel level using the center of gravity of the gradient peak. Similar approach was also used by Ji [Ji et al. (1991)]. Kisworo [Kisworo et al. (1991)] for determination of the subpixel edge position used image energy computed based on image intensity and its Hilbert transform. Interesting approach was also introduced by Bie and Liu [Bie, Liu (2009)]. Their method decomposes pixels into subpixels using quad-tree decomposition.

Having in mind the classification presented above, the method introduced in this paper is the combination of reconstructive and curve fitting methods. More detailed description of the method is given in the following section.

## 3. The Proposed Method

### 3.1. Determination of the Coarse Edge

The proposed method attempts to reconstruct continuous edge information from the discrete image data. In order to diminish the computational complexity of the method the reconstruction is performed in the neighborhood of the edge. Therefore, the method starts from defining the coarse location of the edge. Sobel gradient masks are applied in this step. The input image  $L$  is convolved with the horizontal  $h_x$  and the vertical  $h_y$  mask in accordance with Equation 1.

$$\nabla L \approx \sqrt{(h_x \otimes L)^2 + (h_y \otimes L)^2} \quad (1)$$

The gradient image  $\nabla L$  is next thresholded with a global threshold  $T$ . The value of  $T$  is determined using ISODATA algorithm [Ridler, Calvard (1978)]. Thresholding performed in accordance with Equation 2 produces binary image corresponding with the region of the highest gradient.

$$\nabla L'(x) = \begin{cases} 1 & \text{for } \nabla L(x) \geq T \\ 0 & \text{for } \nabla L(x) < T \end{cases} \quad (2)$$

Finally, the coarse edge is obtained as a result of the skeletonisation performed on the binary image  $|\nabla L'|$  in accordance with Equation 3 [Sidiropoulos et al. (1992)].

$$\delta L = \bigcup_{n=0}^N [(\nabla L' * nH') - (\nabla L' * nH') \circ H] \quad (3)$$

where  $H$  denotes convex structuring element,  $*$  and  $\oplus$  denote erosion and dilation respectively,  $\circ$  denotes morphological opening and:

$$N = \max\{n \mid \nabla L' * nH' \neq \emptyset\} \quad (4)$$

$$H' = \{-h \mid h \in H\} \quad (5)$$

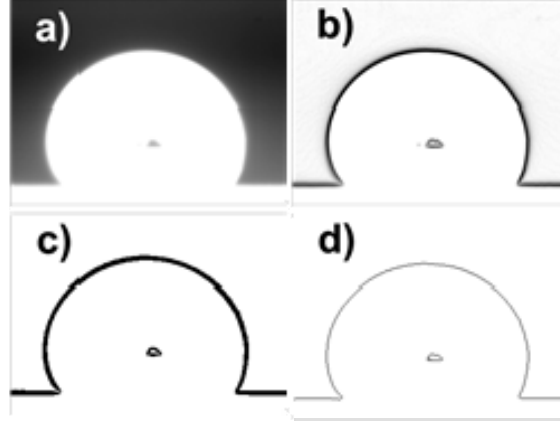


Fig. 1. Successive steps of the coarse border determination; (a) input image; (b) gradient image; (c) image after ISODATA thresholding; (d) coarse edge.

$$nH = \begin{cases} \overline{\{0\}} \oplus H \oplus \dots \oplus H & \text{for } n = 1, 2, \dots \\ \{0\} & \text{for } n = 0 \end{cases} \quad (6)$$

Successive steps of the coarse border determination are presented in Figure 1. Figure 1a presents 8-bit monochromatic image of a specimen of copper at 1031<sup>0</sup>C. Image spatial resolution equals 240 by 320 pixels. In Figure 1b the gradient image is shown. The result of the global ISODATA thresholding is presented in Figure 1c. Finally, Figure 1d presents the coarse border. In order to increase the readability, negatives are shown in Figures 1b-d.

It should be underlined that the method used for the coarse edge determination significantly influences quality of the overall edge detection procedure. It is because the gradient reconstruction is performed only in a close neighbourhood of the coarse edge. The continuous coarse edge can be better refined to subpixel level, as the loss of edge information must be guessed during the edge linking performed in the last step of the algorithm.

### 3.2. Refining Edge to the Subpixel Level

In this step of the algorithm, the reconstruction of gradient profile at the edge is performed. In particular, Gaussian function given by Equation 7 is fitted along the normal direction of edges into a gradient sample values provided by the Sobel operator.

$$f(x) = Ae^{\frac{-(x-\mu)^2}{2\sigma_g^2}} \quad (7)$$

where:  $f(x)$  denotes gradient value at location  $x$ . The linear neighbourhood in the gradient direction is considered. Several pixels on each side of the coarse edge are used. The coordinates of the maximum of the approximating Gaussian function determine edge location with subpixel accuracy.

The fitting is performed in the least-square sense. It aims at determining three parameters of the Gaussian function:

- $\sigma_g$  - which describes the blur level of an edge;
- $A$  - which corresponds with the maximal value of the gradient;
- $\mu$  - which determines the subpixel position of an edge pixel.

The main idea of the subpixel edge detection using the Gaussian function is presented in Figure 2. Discrete data points (empty circles) correspond with gradient sample values (shown under the graph) obtained for pixel at location  $x$ .

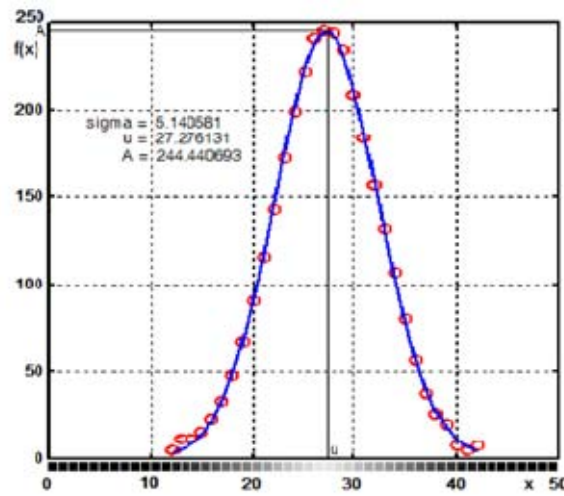


Fig. 2. The main concept of subpixel edge detection using the Gaussian function.

In the previous approaches to subpixel edge detection the trinomial square was used to reconstruct the gradient function. The main advantage of the Gaussian function over the trinomial square is that the first one fits sample gradient values more accurately and produces stable results regardless of the neighbourhood used for gradient reconstruction. The second order polynomial fits gradient function closely only in a small neighbourhood - usually three pixels are used. This makes the method sensitive to noise and blur. The increase of the neighbourhood increases fitting error and makes the reconstructing trinomial square distant from the sample data points. Moreover, the determined subpixel position is unstable as it varies depending on the neighbourhood size. Advantages of the Gaussian function over cubic splines are also noticeable. Specifically, cubic spline interpolation produces function with maximum at a position where gradient perpendicular to the coarse edge reaches maximum. This makes no difference between the coarse and the subpixel edge. This issue is explained in Figure 3. On the consecutive subfigures gradient function reconstructed over the increasing neighbourhood is presented. The horizontal neighbourhood of the pixel  $x(41, 73)$  from Figure 1 is considered. It is assumed that coordinates of the coarse edge pixel are in the centre of this pixel and equal  $(41.5, 73.5)$ . Empty circles indicate gradient sample values. Solid line represents the

approximating Gaussian function. Dashed line relates to the reconstructing trinomial square. Finally, dash-dotted line shows the determined cubic spline. The size of the neighbourhood considered during the gradient reconstruction equals respectively: 3 (Fig. 3a), 5 (Fig. 3b), 7 (Fig. 3c), 11 (Fig. 3d), 15 (Fig. 3e) and 19 (Fig. 3f) pixels. Gradient function at location  $x$  is denoted as  $f(x)$ .

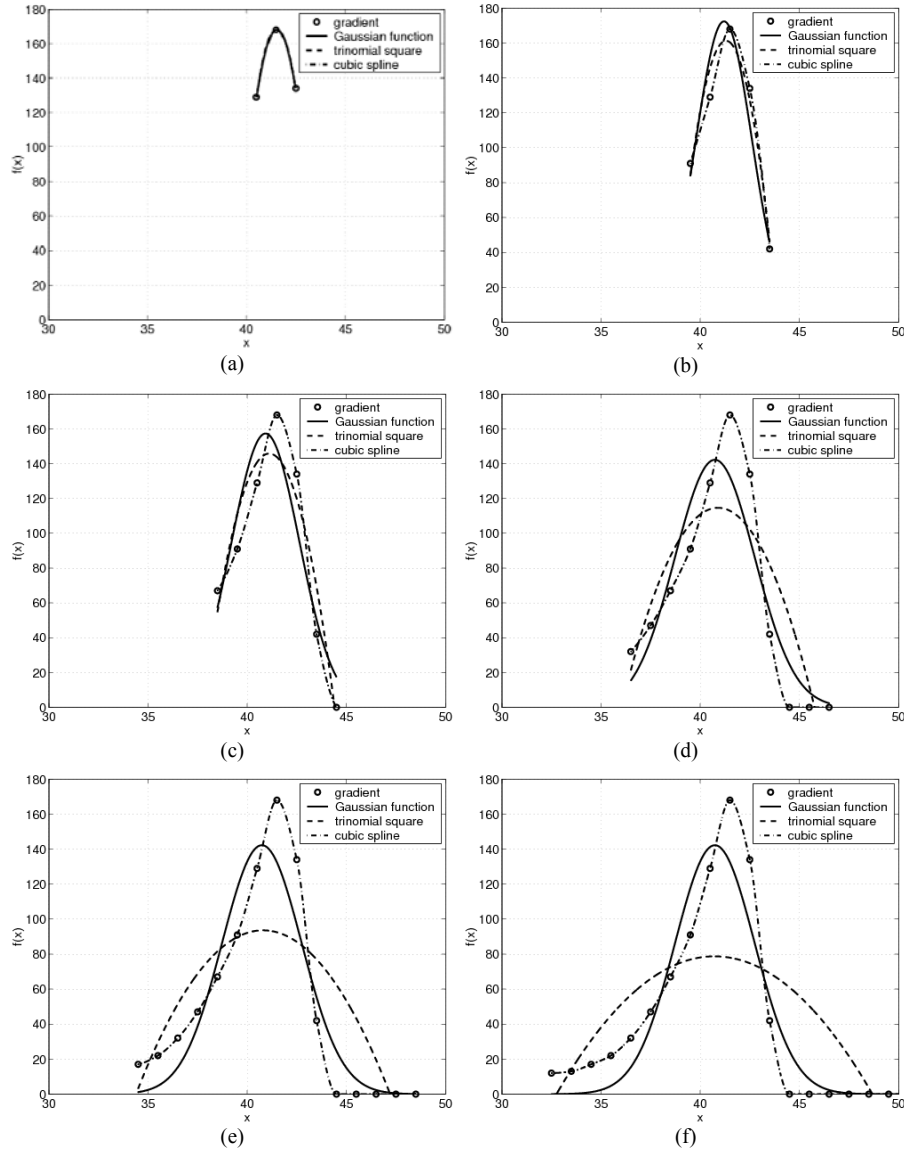


Fig. 3. The influence of the neighbourhood size used for gradient reconstruction on the shape of the resulting function and the determined subpixel edge position; (a) neighbourhood: 3 pixels; (b) neighbourhood: 5 pixels; (c) neighbourhood: 7 pixels; (d) neighbourhood: 11 pixels; (e) neighbourhood: 15 pixels; (f) neighbourhood: 19 pixels.



The subpixel position of the considered edge pixel obtained for the corresponding functions from Figure 3 is given in Table 1. In the first column (N.Size) the size of the neighbourhood used for gradient reconstruction is indicated. The size is given in pixels. In the second column (Gauss.) the subpixel position provided by the Gaussian function is given. Columns third (TS) and fourth (CS) show the results provided by the trinomial square and the cubic spline respectively. Additional information is given in the fifth column (GC) which presents subpixel position of the considered edge pixel obtained using the gravity centre approach proposed by [Stanke et al. (1998)].

Table 1. The subpixel position of the considered edge pixel determined for the increasing neighbourhood using various methods; N.Size - the size of the neighbourhood; Gauss. - Gaussian function; TS - trinomial square; CS - cubic spline; GC - gravity centre.

| N.Size | Gauss.  | TS      | CS      | GC      |
|--------|---------|---------|---------|---------|
| 3      | 41.5388 | 41.5300 | 41.5000 | 41.5116 |
| 5      | 41.1991 | 41.3000 | 41.5000 | 41.3351 |
| 7      | 40.9244 | 41.1100 | 41.5000 | 41.0341 |
| 9      | 40.7396 | 40.9800 | 41.5000 | 40.7891 |
| 11     | 40.7396 | 40.9000 | 41.5000 | 40.5958 |
| 13     | 40.7396 | 40.8500 | 41.5000 | 40.4426 |
| 15     | 40.7396 | 40.8000 | 41.5000 | 40.3077 |
| 17     | 40.7396 | 40.7600 | 41.5000 | 40.1916 |
| 19     | 40.7396 | 40.7200 | 41.5000 | 40.0724 |
| 21     | 40.7396 | 40.6800 | 41.5000 | 39.9630 |

The results presented in Figure 3 and Table 1 prove superiority of the Gaussian function over the previously used approaches. Interpolation using cubic spline is useless. The remaining approaches to subpixel approach (i.e. the trinomial square approximation and the gravity centre approach) produce results which depend on the size of the neighbourhood used for gradient reconstruction. This makes them ambiguous and requires additional criteria indicating size of the neighbourhood which should be used. Therefore choosing the Gaussian function for gradient approximation appears to be the most appropriate in terms of the stability of the determined subpixel edge position.

### 3.3. Edge Linking

In the last step of the algorithm, the edge linking can be performed. This step is optional. It aims at obtaining continuous border from the edge points determined in the previous step with subpixel accuracy.

Firstly, the coarse edge is represented by means of chain code i.e. the connected sequence of straight-line segments of a specified length and direction; 8-connectivity segments are considered [Gonzalez, Woods (2007)]. Despite the information about the succeeding pixel, each node of the chain contains information about the corresponding subpixel position. Next, Cubic B-spline interpolation is performed over the subpixel positions corresponding with consecutive pixels in the chain code.

## 4. Tests on Simulated Data

### 4.1. Blur Resistance

Firstly, the proposed method for subpixel edge detection was tested on the simulated data. Specifically, the robustness of the method against the Gaussian blur and the averaging was investigated. In order to present robustness of the Gaussian function in determining blurred edge position, the third step of the algorithm (i.e. edge linking) was not performed on the presented results.

Geometrically created 8-bit grayscale image of a circle was used to test the performance of the proposed approach. The circle of radius 50 pixels was centred at the position (75.0, 75.0). The intensity of the background was 52 while the intensity of the circle was 255.

The assessment of edge detection quality was made by means of:

- the coordinates of the determined circle centre;
- the radius of the determined circle;
- the standard deviation of the radius of the determined circle.

Coordinates of the circle centre were defined as the gravity centre of the determined subpixel edge points and computed in accordance with the Equation 8.

$$\begin{cases} x_c = \frac{1}{n} \sum_{i=1}^n x_i \\ y_c = \frac{1}{n} \sum_{i=1}^n y_i \end{cases} \quad (8)$$

where  $n$  is the number of subpixel edge points and  $x_i, y_i$  denote coordinates of  $i$ -th subpixel edge point.

The radius is defined as the average distance of subpixel edge points from the real circle center (i.e. (75.0, 75.0)). This is expressed by Equation 9.

$$\bar{r} = \frac{1}{n} \sum_{i=1}^n \sqrt{(75.0 - x_i)^2 + (75.0 - y_i)^2} \quad (9)$$

The test image was distorted by:

- the Gaussian filter of an increasing radius (from 1 to 10);
- the averaging filter of an increasing size (from 1 to 10).

The results of edge detection in images distorted by Gaussian blur are presented in Figures 4 and 5. In particular, Figure 4 shows edges obtained with the subpixel accuracy rounded to the closest pixel. The results of the proposed method were compared with results provided by the Sobel operator, the gravity centre approach and the trinomial square (parabola) fitting approach. The Gaussian function was fitted into 21-pixel neighbourhood in order to ensure position of reconstructing function peak becomes stable. This neighbourhood was also used to compute the centre of gravity. Parabola was fitted into 5-pixel neighbourhood to ensure close fitting. The method used for edge detection is indicated above each column. The radius of the Gaussian filter used for blurring is given at the beginning of each row.

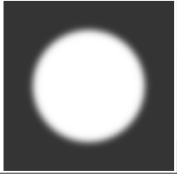
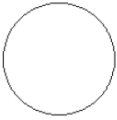
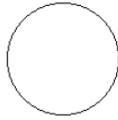
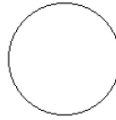
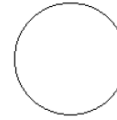


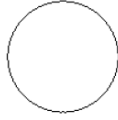
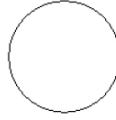
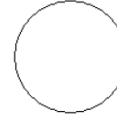
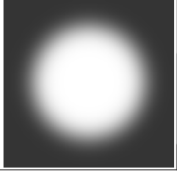

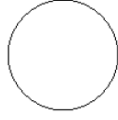
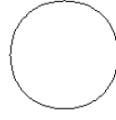

|                           |   | ORIGINAL IMAGE  | SOBEL   | PROPOSED APPROACH   | GRAVITY CENTER   | PARABOLA FITTING  |
|---------------------------|---|---|---|---|--|---|
| RADIUS OF GAUSSIAN FILTER | 3 |  |  |  |  |  |
|                           | 6 |  |  |  |  |  |
|                           | 9 |  |  |  |  |  |

Fig. 4. The results of edge detection at the subpixel level in images distorted by the Gaussian blur.

Figure 5 compares the results of edge detection at the subpixel level. The proposed method, Sobel operator, the gravity centre approach and the trinomial square (parabola) fitting approach are considered again. Specifically, Figure 5a shows the error of circle centre determination in function of radius of the Gaussian filter used for blurring. The error is expressed by means the Euclidean distance between the real and the determined (in accordance with Eq. 8) circle centre. Figure 5b presents the error of circle radius determination in function of radius of the Gaussian filter used for blurring. The error is expressed by means the difference in length between the real and the determined (in accordance with Eq. 9) radius. Finally, Figure 5c presents the standard deviation of the circle radius in function of radius of the Gaussian filter used for blurring.

The results of edge detection in images distorted by the averaging filter are presented in Figures 6 and 7 and are organized as previously. Figure 6 shows edges obtained with the subpixel accuracy rounded to the closest pixel. Figure 7 presents a comparison of edge detection results at subpixel level. In particular, Figure 7a shows the error of circle centre determination in the function of the size of an averaging filter used for blurring. Figure 7b presents the error of circle radius determination in the function of the size of an averaging filter used for blurring. Finally, Figure 7c presents the standard deviation of the circle radius in the function of size of an averaging filter used for blurring.

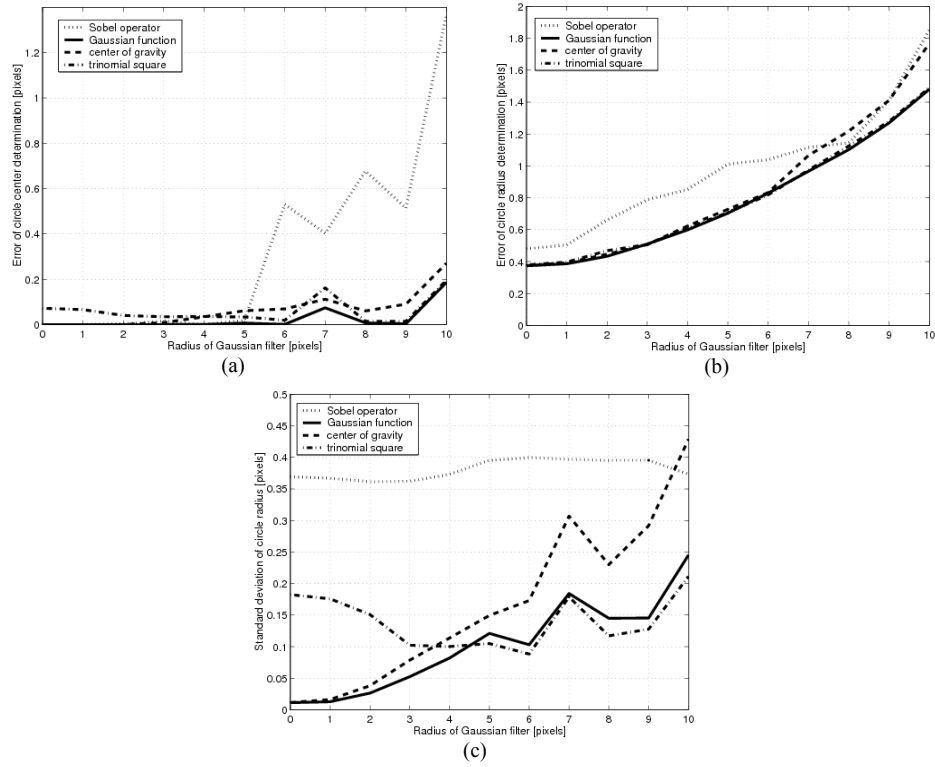


Fig. 5. The results of edge detection at subpixel level in images distorted by the Gaussian blur; (a) circle centre error; (b) radius error; (c) standard deviation of radius.

|                          |   | ORIGINAL IMAGE | SOBEL | PROPOSED APPROACH | GRAVITY CENTER | PARABOLA FITTING |
|--------------------------|---|----------------|-------|-------------------|----------------|------------------|
| SIZE OF AVERAGING FILTER | 3 |                |       |                   |                |                  |
|                          | 6 |                |       |                   |                |                  |
|                          | 9 |                |       |                   |                |                  |

Fig. 6. The results of edge detection at the subpixel level in images distorted by averaging filter.

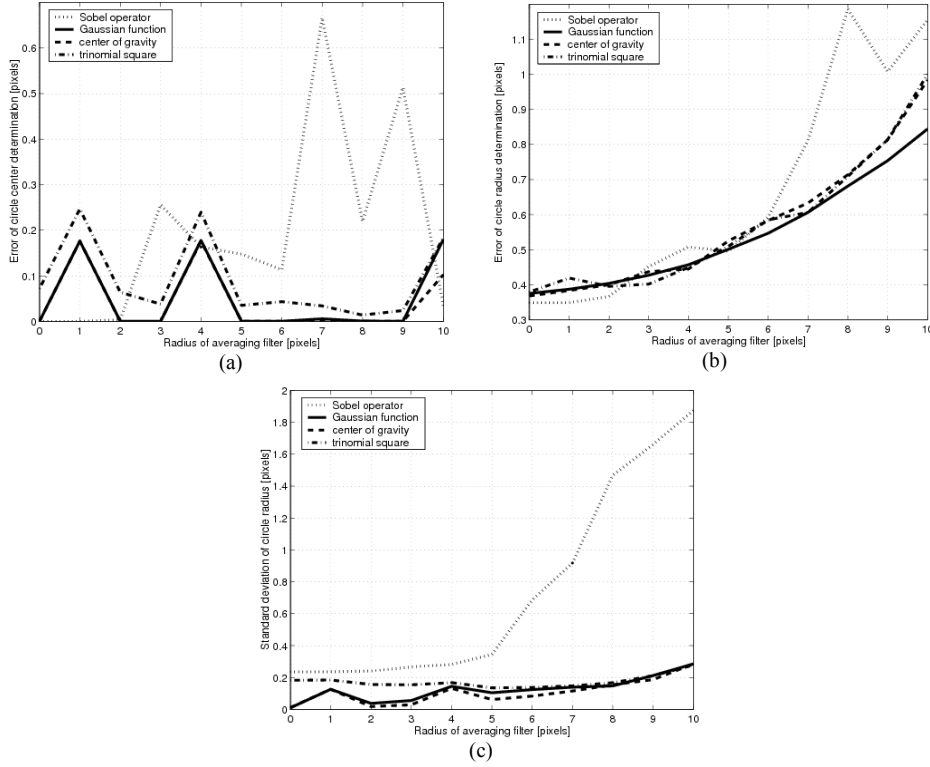


Fig. 7: The results of edge detection at subpixel level in images distorted by an averaging filter; (a) circle center error; (b) radius error; (c) standard deviation of radius.

The results presented in Figures 4-7 prove the robustness of the proposed method against the Gaussian blur and the averaging. In order to present robustness of Gaussian function in determining blurred and noisy edge position, the third step of the algorithm (i.e. edge linking) was not performed on the presented results.

In the case of images distorted by the Gaussian blur the proposed method significantly outperforms other regarded methods for subpixel edge detection. The superiority of the Gaussian function based approach can be observed even at pixel level, as the method provides continuous, regular and most circular edges. The trinomial square fitting approach fails to produce continuous and sharp edges - especially for the large blur. The gravity centre approach produces continuous edges. However object shape is changed. It can be observed that for the large blur the determined edges become squarer. The results obtained at subpixel level also confirm the superiority of the proposed method. In the case of the considered test images (over a wide range of the Gaussian blur) the method provides the smallest errors of circle centre determination and circle radius determination. Moreover, it ensures the lowest standard deviation of the circle radius what proves the highest regularity of the determined edges.

In the case of images distorted by an averaging filter Gaussian function based approach significantly outperforms the trinomial square fitting approach which produces unsharp (discontinuous) edges and remarkably influences object shape. The advantage over the gravity centre approach is slight and can be observed mainly in the case of circle radius determination.

Nevertheless, the results obtained for the synthetic images prove correctness of the introduced method, its robustness against blurred edges and its superiority over other approaches to subpixel edge detection.

#### 4.2. Noise Resistance

In order to test the performance of the proposed algorithm with respect to noise, the geometrically created image of a circle (described in the previous section) after blurring was corrupted by Gaussian noise of an increasing standard deviation  $\sigma$ . Images under a wide range of corruption were considered. Specifically, value of  $\sigma$  was changed from 5 to 50 with a step of 5.

Because the noise presence significantly influences regularity of the proposed method the assessment of edge detection quality was made by means of parameters of a circle fitted into the determined subpixel edge points. In particular, the coordinates of the circle centre and its radius were considered. The circle was fitted into the determined subpixel edge points in least-square sense.

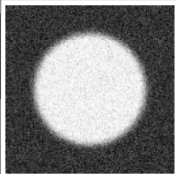
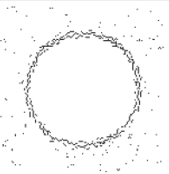
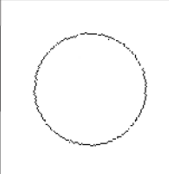
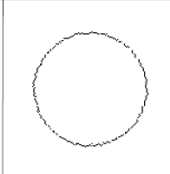

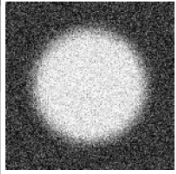
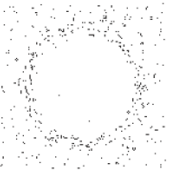

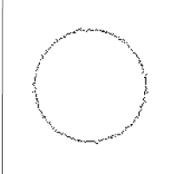
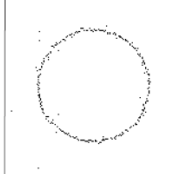
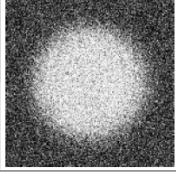
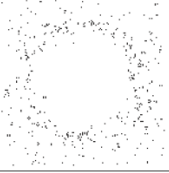

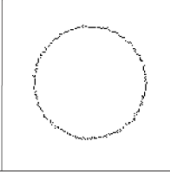
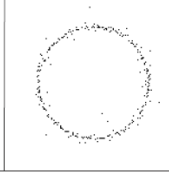
|                          | ORIGINAL IMAGE  | SOBEL   | PROPOSED APPROACH   | GRAVITY CENTER   | PARABOLA FITTING  |
|--------------------------|---|---|---|--|---|
| Radius = 3<br>Sigma = 20 |  |  |  |  |  |
| Radius = 6<br>Sigma = 35 |  |  |  |  |  |
| Radius = 9<br>Sigma = 50 |  |  |  |  |  |

Fig. 8: The results of edge detection at subpixel level in images distorted by the Gaussian blur and the Gaussian noise.

The results of edge detection in the selected noisy images are presented in Figure 8. Three images were used: (i) the image blurred with the Gaussian filter of radius equal 3

corrupted by noise of the standard deviation  $\sigma$  equal 20, (ii) the image blurred with the Gaussian filter of radius equal 6 corrupted by noise of the standard deviation  $\sigma$  equal 35 and (iii) the image blurred with the Gaussian filter of the radius equal 9 corrupted by noise of the standard deviation  $\sigma$  equal 50. The input images are presented in the first column. The results obtained with the proposed approach are compared with the results provided by the Sobel edge detector, the gravity centre approach and the trinomial square (parabola) fitting approach. The method used for edge detection is indicated above each column.

The comparison of edge detection in blurry and noisy images at subpixel level is presented in Figure 9. In particular, the graphs show the error of the circle center determination (the first row) and the circle radius determination (the second row) in function of the standard deviation of the Gaussian noise. Figure 9a corresponds with the results of edge detection in images blurred by the Gaussian filter of radius equal, Figure 9b corresponds with the results of edge detection in images blurred by the Gaussian filter of radius equal 6 and Figure 9c corresponds with the results of edge detection in images blurred by the Gaussian filter of radius equal 9. The error of the circle center and the circle radius was determined as described in Section 4.1.

The results presented in Figures 8 and 9 show that the proposed method successfully detects edges also in noisy images. The Gaussian function can be adjusted to match gradient at significantly blurred and noisy images what allows to obtain high precision of edge detection.

The advantage of the proposed method over the trinomial square (parabola) fitting approach can be seen at pixel level. Parabola can not be fitted properly into the blurry and noisy edge what results with unsharp and irregular edge.

The advantage of the proposed method over the gravity centre approach can be observed at subpixel level (see Fig. 9). However, it is not as obvious as in the case of the trinomial square fitting approach. The analysis of errors of the circle centre and the circle radius brings a conclusion that the proposed approach produces lower errors for a wider range of noise corruption than the gravity centre approach. On this basis it can be judged that the proposed Gaussian function based method outperforms the gravity centre approach also in case of images corrupted by noise.

## 5. Tests on Real Data

In the next step, the tests with real images were performed in order to define the scope of applicability of the introduced method for the subpixel edge detection. In particular, images of heat-emitting specimens of metals and alloys obtained from the computerized system for high temperature measurements of surface properties [Sankowski et al. (2000); Fabijańska, Sankowski (2008)] were considered. Due to the intense thermal radiation, usage of gas protective atmosphere and application of infra-red filters these images are characterized by low contrast and blurred edges.

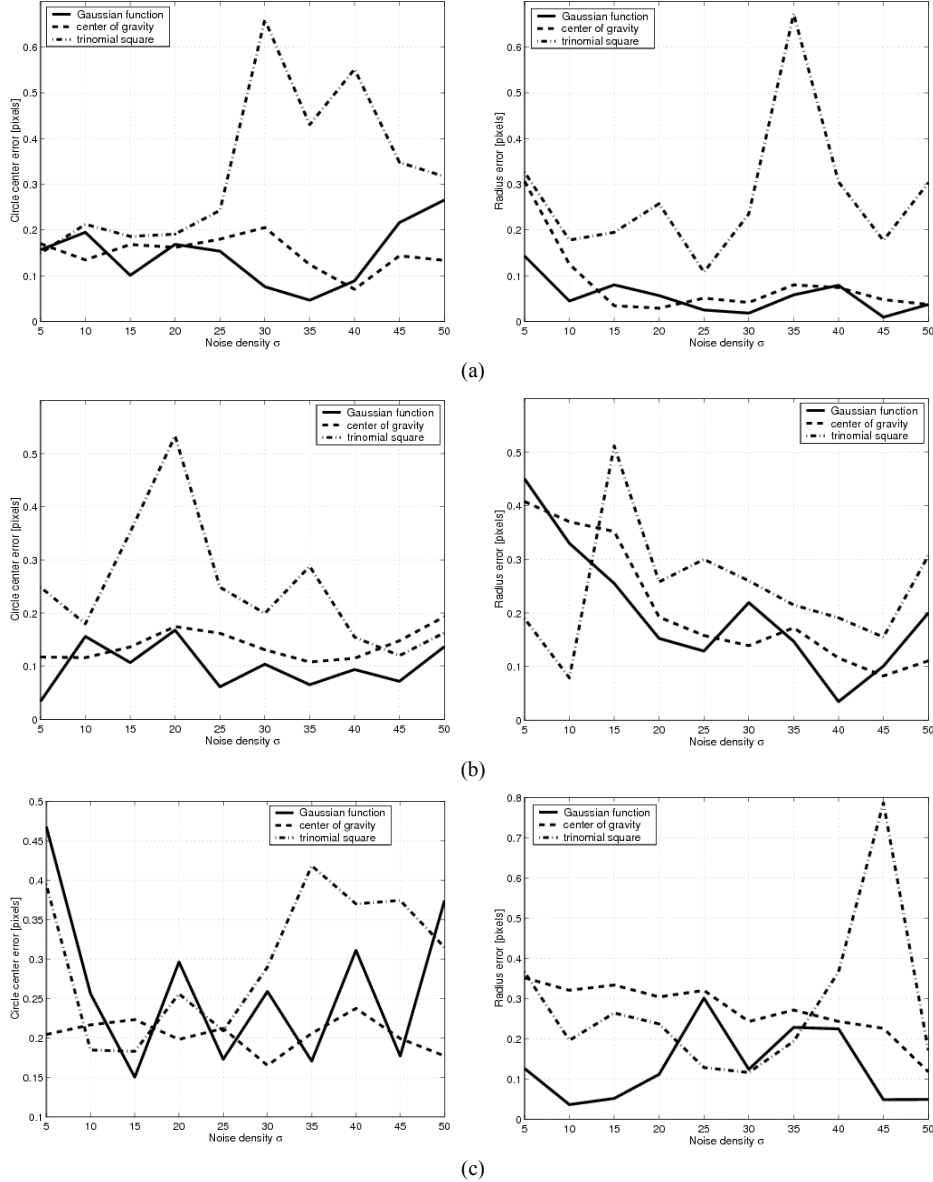


Fig. 9. The results of edge detection at subpixel level in images distorted by Gaussian blur and Gaussian noise; (a) radius of Gaussian filter: 3; (b) radius of Gaussian filter: 6; (c) radius of Gaussian filter: 9.

The results of edge detection in images of different specimens are presented in Figure 10. In the first column the original images are presented. They present respectively specimen of steel at 1104<sup>0</sup>C, specimen of steel at 1311<sup>0</sup>C, specimen of copper at 853<sup>0</sup>C and specimen of copper at 1265<sup>0</sup>C. Images were obtained with various infra-red filters. The second column shows the corresponding results of edge detection



obtained by Sobel gradient operator. The third column presents the results of refining Sobel coarse edges to subpixel level using the Gaussian function. Finally, the last column presents the results obtained using the complete introduced procedure of subpixel edge detection. In order to present robustness of the Gaussian function in determining blurred edge position, the third step of the algorithm (i.e. edge linking) was not performed on the presented results.

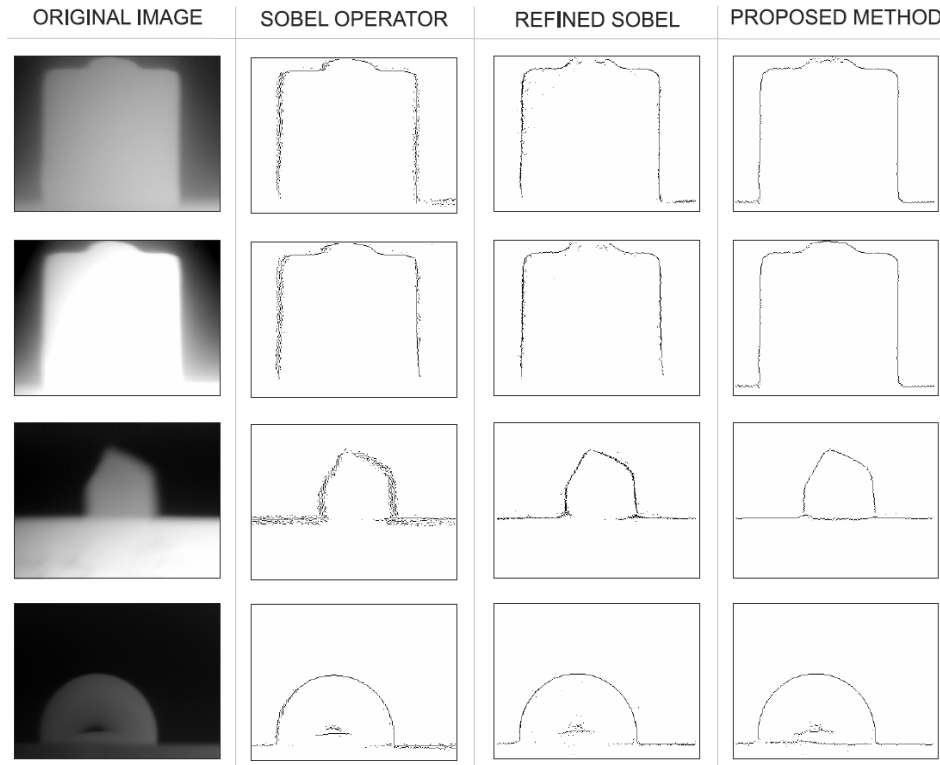


Fig. 10. The results of edge detection using Gaussian function based approach compared to results provided by Sobel gradient operator.

The results shown in Figure 10 show clearly, that the proposed method significantly improves quality of edge detection in images of heat-emitting specimens of metals and alloys.

In the case of the considered class of low contrast images Sobel operator produces wide, irregular and ambiguous edges. Such accuracy is unacceptable. Refining Sobel edge to subpixel level using Gaussian function remarkably improves the precision of edge location. Edges become more compact and regular. However, the accuracy of edge detection is still limited by the accuracy of Sobel operator used for the coarse edge determination. The most significant increase in edge detection accuracy can be observed when the complete introduced procedure is applied. The proposed method for coarse edge determination is less sensitive to noise and other distortions than the traditional

Sobel approach. As a result it produces the unequivocal, one-pixel width coarse edge which can be better refined by the Gaussian function. Subpixel edges produced by the introduced method are remarkably more regular. Moreover, they are significantly more continuous what diminishes the amount of edge information to be guessed during edge linking and makes the results more unequivocal.

## 6. Conclusions

In this paper the problem of edge detection at subpixel level was considered. In particular, the precise edge detection in blurred and noisy images was regarded. The reconstructive method for subpixel edge detection was introduced. The method firstly determines the coarse edge using Sobel gradient masks, thresholding and skeletonisation. Then, it attempts to reconstruct continuous image gradient function at the coarse edge using the Gaussian function. The position of the maximum of the reconstructing Gaussian function indicates the edge with subpixel accuracy.

The correctness and robustness of the method was proven by tests performed on geometrically created synthetic images under a wide range of blur and noise corruption. Obtained results clearly show that the proposed method significantly improves quality of edge detection. The refined edges are continuous and much more regular than those provided by the traditional Sobel gradient masks. The more blurred and noisy is the edge, the difference is more significant. Moreover, the proposed method outperforms other approaches for subpixel edge detection i.e. gravity centre approach and trinomial square fitting approach. The advantage of the Gaussian function based method can be seen both: in the accuracy and the stability of the obtained subpixel edge position.

Tests performed on the real images obtained from high temperature industrial vision system prove that the introduced method can be particularly useful in the case of low contrast images with blurred and unsharp edges. In consequence it can be successfully applied in a wide spectrum of machine vision applications where accuracy is at premium.

## References

- Bailey, D. G. (2005): Sub-pixel Profiling. Proc. 5th Int. Conf. Information Communications and Signal Processing: 1311–1315.
- Bie, X. H. and Liu, C. Y. (2009): Edge-Directed Sub-Pixel and Still Image Super-Resolution. Proc. 2nd Int. Cong. Image and Signal Processing: 1–4.
- Bin, T. J., Lei, A., Jiwen, C., Wenjing, K. and Dandan, L. (2008): Subpixel Edge Location Based On Orthogonal Fourier-Mellin Moments. Image Vision Comput., 26(4): 563–569.
- Breder, R., Estrela, V. V. and de Assis, J. T. (2009): Sub-Pixel Accuracy Edge Fitting by Means of B-Spline. Proc. IEEE. Int. Workshop Multimedia Signal Processing: 1–5.
- Fabijańska, A. and Sankowski, D. (2008): Computer Vision System for High Temperature Measurements of Surface Properties. Mach. Vision Appl., 20(6): 411–421.
- Fabijańska, A. (2012): A Survey of Subpixel Edge Detection Methods on Images of Heat-Emitting Metal Specimens. Int. J. Appl. Math. Comp., 22(3): 695–710.
- Fabijańska, A. (2014): Gaussian-Based Approach to Subpixel Detection of Blurred and Unsharp Edges, Proc. Federated Conference on Computer Science and Information Systems: 647–656.
- Ghosal, S. and Mehrotra, R. (1993): Orthogonal Moment Operators for Subpixel Edge Detection. Pattern Recogn. Lett., 26(2): 295–305.

- Gonzalez, R. C and Woods, R. E. (2007): Digital Image Processing 3rd Edition
- Hagara, M. and Kulla, P. (2011): Edge Detection with Sub-pixel Accuracy Based on Approximation of Edge with Erf Function. *Radioengineering*, 20(2): 516–524
- Ji, X., Wang, K. and Wei, Z. (1991): Structured Light Encoding Research Based on Sub-Pixel Edge Detection. *Proc. Int. Conf. Information Engineering and Computer Science*: 1–4.
- Jin, J. S. (1990): An Adaptive Algorithm for Edge Detection with Subpixel Accuracy in Noisy Images. *Proc. IAPR Workshop on Machine Vision Applications*: 249–252.
- Kisworo, M., Venkatesh, S. and West, G. (1991): 2-D Edge Feature Extraction To Subpixel Accuracy Using the Generalized Energy Approach. *Proc. IEEE Region 10 Int. Conf. EC3-Energy Computer, Communication and Control Systems*: 344–348.
- Liu, C., Xia, Z., Niyokindi, S., Pei, W., Song, J. and Wang, L. (2004): Edge Location to Sub-Pixel Value in Color Microscopic Images. *Proc. Int. Conf. Intelligent Mechatronics and Automation*: 548–551.
- Lyvers, E. P., Mitchell, O. R., Akey, M. L. and Reeves, A. P. (1989): Subpixel Measurements Using a Moment-Based-Edge Operator. *IEEE Trans. Pattern Anal. Mach. Intell.*, 11(12): 1293–1309.
- Machuca, R. and Gilbert, A. L. (1981): Finding Edges in Noisy Scenes. *IEEE Trans. Pattern Anal. Mach. Intell.*, PAMI-3: 103–111.
- MacVicar-Whelan, P. J. and Binford, T. O. (1981): Line Finding with Subpixel Precision. *Proc. DARPA Image Understanding Workshop*: 26–31.
- MacVicar-Whelan, P. J. and Binford, T. O. (1991): Intensity Discontinuity Location to Subpixel Precision. *Proc. Int. Joint Conf. Artificial Intelligence*: 26–31.
- Nevtia, R. and Babu, K. (1978): Linear Feature Extraction. *Proc. DARPA Image Understanding Workshop*: 73–78.
- Ridler, T. and Calvard, S. (1978): Picture Thresholding Using an Iterative Selection Method. *IEEE Trans. Syst. Man Cybern. Syst.* 8: 630–632.
- Rocket, P. (1999): The Accuracy of Sub-Pixel Localization in the Canny Edge Detector. *Proc. British Machine Vision Conf.*: <http://www.bmva.org/bmvc/1999/papers/39.pdf> (accessed on Jan 2015).
- Sankowski, D., Strzecha K., Jezewski, S. (2000): Digital Image Analysis in Measurement of Surface Tension and Wettability Angle. *Proc. Int. Conf. Modern Problems of Telecommunications, Computer Science and Engineers Training*: 129–130.
- Sheng, Y. and Shen, L. (1994): Orthogonal Fourier-Mellin Moments for Invariant Pattern Recognition. *J. Opt. Soc. Am.*, 11(6): 1748–1757.
- Sidiropoulos, N. D., Baras, J. S. and Berenstein, C. A. (1992): Discrete Random Sets: An Inverse Problem, Plus Tools for the Statistical Inference of the Discrete Boolean Model. *Proc. SPIE*, 1769: 32–43.
- Stanke, G., Zedler, L., Zorn, A., Weckend, F. and Weide, H. G. (1998): Sub-Pixel Accuracy by Optical Measurement of Large Automobile Components. *Proc. 24th Annual Conf. of IEEE Industrial Electronics Society*: 2431–2433.
- Tabatabai, A. J. and Mitchell, O. R. (1984): Edge Location to Sub-Pixel Values in Digital Imagery. *IEEE Trans. Pattern Anal. Mach. Intell.*, 6(2): 188–201.
- Xu, G. S. (2009): Sub-pixel Edge Detection Based on Curve Fitting. *Proc. 2nd Int. Conf. Information and Computing Science*: 373–375.
- Xu, G. S. (2009b): Linear Array CCD Image Sub-pixel Edge Detection Based on Wavelet Transform. *Proc. 2nd Int. Conf. Information and Computing Science*: 204–206.
- Yao, Y. and Ju, H. (2009). A Sub-Pixel Edge Detection Method Based on Canny Operator. *Proc. 6th Int. Conf. Fuzzy Systems and Knowledge Discovery*: 97–100.